Journal Pre-proof

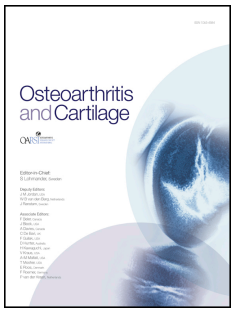

Identification of TGFβ signatures in six murine models mimicking different osteoarthritis clinical phenotypes

Marie Maumus, PhD, Danièle Noel, PhD, Hang Korng Ea, MD-PhD, David Moulin, PhD, Maxime Ruiz, PhD, Eric Hay, PhD, Xavier Houard, PhD, Damien Cleret, PhD, Martine Cohen-Solal, MD-PhD, Claire Jacques, PhD, Jean-Yves Jouzeau, MD-PhD, Marie-Hélène Lafage-Proust, MD-PhD, Pascal Reboul, PhD, Jérémie Sellam, MD-PhD, Claire Vinatier, PhD, François Rannou, MD-PhD, Christian Jorgensen, MD-PhD, Jérome Guicheux, Francis Berenbaum, MD-PhD

PII: S1063-4584(20)31059-1

DOI: https://doi.org/10.1016/j.joca.2020.06.008

Reference: YJOCA 4688

To appear in: *Osteoarthritis and Cartilage*

Received Date: 4 March 2020

Revised Date: 12 June 2020

Accepted Date: 22 June 2020

Please cite this article as: Maumus M, Noel D, Ea HK, Moulin D, Ruiz M, Hay E, Houard X, Cleret D, Cohen-Solal M, Jacques C, Jouzeau J-Y, Lafage-Proust M-H, Reboul P, Sellam J, Vinatier C, Rannou F, Jorgensen C, Guicheux J, Berenbaum F, Identification of TGFβ signatures in six murine models mimicking different osteoarthritis clinical phenotypes, *Osteoarthritis and Cartilage*, https://doi.org/10.1016/j.joca.2020.06.008.

Identification of TGFβ signatures in six murine models mimicking different osteoarthritis clinical phenotypes

Marie MAUMUS PhD[1], Danièle NOEL PhD[1,2,*], Hang Korng EA MD-PhD[3], David MOULIN PhD[4], Maxime RUIZ PhD[1], Eric HAY PhD[3], Xavier HOUARD PhD[5], Damien CLERET PhD[6], Martine COHEN-SOLAL MD-PhD[3], Claire JACQUES PhD[5], Jean-Yves JOUZEAU MD-PhD[4,7], Marie-Hélène LAFAGE-PROUST MD-PhD[6], Pascal REBOUL PhD[4], Jérémie SELLAM MD-PhD[5,8], Claire VINATIER PhD[9,10], François RANNOU MD-PhD[11], Christian JORGENSEN MD-PhD[1,2], Jérome GUICHEUX[9,10,12,#], Francis BERENBAUM MD-PhD[5,8,#]

[1]IRMB, University of Montpellier, INSERM, Montpellier, France; [2]Clinical immunology and Osteoarticular diseases Therapeutic Unit, Hôpital Lapeyronie, Montpellier, France; [3]Université de Paris, BIOSCAR Inserm U1132, and Department of rheumatology, AP-HP, Hôpital Lariboisière, Paris, France; [4]Université de Lorraine, UMR 7365 CNRS, Ingénierie Moléculaire et Physiopathologie Articulaire (IMoPA), Vandœuvre Les Nancy, France; [5]Sorbonne Université, INSERM, Centre de Recherche Saint-Antoine, Paris, France; [6]INSERM U1059, Universite J Monnet @ Universite De Lyon , CHU, Saint-Etienne, France; [7]Laboratoire de Pharmacologie Clinique et Toxicologie, Centre Hospitalier Régional Universitaire de Nancy, Vandœuvre Les Nancy, France; [8]Department of Rheumatology, AP-HP Saint- Antoine Hospital, DMU 3iD, Paris, France; [9]Inserm, UMR 1229, RMeS, Regenerative Medicine and Skeleton, Université de Nantes, ONIRIS, Nantes, France; [10]Université de Nantes, UFR Odontologie, Nantes, France; [11]INSERM UMR-S 1124, Toxicité Environnementale, Cibles Thérapeutiques, Signalisation Cellulaire et Biomarqueurs, Faculté des Sciences Fondamentales et Biomédicales, Université de Paris, Sorbonne Paris Cité, Paris, and AP-HP, Groupe Hospitalier AP-HP. Centre-Université de Paris, Hôpital Cochin, Service de Rééducation et de Réadaptation de l'Appareil Locomoteur et des Pathologies du Rachis, Paris, France. Université de Paris, Faculté de Santé, UFR Médecine Paris Descartes, Paris, France; [12]CHU Nantes, PHU4 OTONN, Nantes, France

[#]: equally contributing authors

Running title: TGFβ expression in 6 murine models of OA

* Corresponding author: Danièle Noël

Inserm U1183, IRMB, Hôpital Saint-Eloi,

80 avenue Augustin Fliche, 34295 Montpellier cedex 5, France

Tel: +33 4 67 33 04 73 - Fax: +33 4 67 33 01 13 - E-mail: daniele.noel@inserm.fr

Objective. TGFβ is a key player in cartilage homeostasis and OA pathology. However, few data are available on the role of TGFβ signalling in the different OA phenotypes. Here, we analysed the TGFβ pathway by transcriptomic analysis in six mouse models of OA.

Method. We have brought together seven expert laboratories in OA pathophysiology and, used inter-laboratories standard operating procedures and quality controls to increase experimental reproducibility and decrease bias. As none of the available OA models covers the complexity and heterogeneity of the human disease, we used six different murine models of knee OA: from post-traumatic/mechanical models (meniscectomy (MNX), MNX and hypergravity (HG-MNX), MNX and high fat diet (HF-MNX), MNX and seipin knock-out (SP-MNX)) to aging-related OA and inflammatory OA (collagenase-induced OA (CIOA)). Four controls (MNX-sham, young, SP-sham, CIOA-sham) were added. OARSI-based scoring of femoral condyles and RNA extraction from tibial plateau samples were done by single operators as well as the transcriptomic analysis of the TGFβ family pathway by Custom TaqMan® Array Microfluidic Cards.

Results. The transcriptomic analysis revealed specific gene signatures in each of the six models; however, no gene was deregulated in all six OA models. Of interest, we found that the combinatorial *Gdf5-Cd36-Ltbp4* signature might discriminate distinct subgroups of OA: *Cd36* upregulation is a hallmark of MNX-related OA while *Gdf5* and *Ltbp4* upregulation is related to MNX-induced OA and CIOA.

Conclusion. These findings stress the OA animal model heterogeneity and the need of caution when extrapolating results from one model to another.

Keywords: osteoarthritis, signature, murine model, transcriptomic

A collaborative study between 7 expert laboratories in osteoarthritis pathophysiology rose the challenge to identify common gene signatures in six murine models of osteoarthritis representative of clinical phenotypes in osteoarthritic patients using standard operating procedures and centralized analyses.

The main findings of the study are the absence of one common deregulated gene in all six osteoarthritis models but the identification of a combinatorial *Gdf5*-*Cd36*-*Ltbp4* signature that might discriminate distinct subgroups of OA.

INTRODUCTION

Although osteoarthritis (OA) is the most prevalent joint disease worldwide, there is still not a single disease-modifying OA drug on the market. The current treatment options usually result in poorly predictable outcomes due to the high interpatient variability in OA clinical and structural features. Indeed, some studies have reported OA phenotype heterogeneity among patients [1-3]. Recently it has been proposed to use advanced techniques to identify combinatorial biomarkers for distinguishing the different OA phenotypes [4], and also to identify patients at higher risk of disease progression, or with different underlying pathophysiologic mechanisms and risk factors [5]. This will help to improve clinical research and to develop targeted treatments and prevention strategies based on a phenotype-guided approach. The advantage of searching for targets based on differences between risk factors is the simplicity then of selecting patients for future personalized medicine.

Currently, OA research relies on the use of various animal models (mainly mice and rats, and more rarely large animals) that mimic mechanical, metabolic or inflammatory OA. However, none of these models covers the complexity and heterogeneity of the human disease but different models likely reflect the heterogeneity of human OA. Moreover, it is difficult to compare the results of different experimental studies due to the heterogeneity of animal backgrounds and experimental protocols. Several studies have analysed global gene expression in OA samples using RNA-seq [6-8] and have generated huge amounts of datasets. However, only small subsets of data are validated and large amounts of data are commonly not investigated. To try to tackle some of these limitations, seven French academic laboratories experts in OA animal models formed a Research on OsteoArthritis Disease (ROAD) consortium to centralize many experimental steps and to put in place

standard operating procedures (SOP) in order to minimize bias and increase reproducibility. The first objective of the ROAD consortium was to investigate the TGFβ pathway in various OA phenotypes. Indeed, recent findings have shown that TGFβ is a central player in cartilage homeostasis and OA pathology [9]. However, few data are available on the pathophysiological role of TGFβ family members in the different OA phenotypes. Therefore, the consortium analysed the TGFβ pathway by transcriptomic analysis in six murine models of knee OA that reproduce the main phenotypes of the human disease: surgical meniscectomy (MNX) to mimic mechanical or post-traumatic OA, hypergravity and MNX (HG-MNX) to mimic overweight-induced mechanical OA, high fat diet and MNX (HF-MNX) to mimic obesity-induced OA, seipin knock-out and MNX (SP-MNX) to mimic metabolic syndrome-induced OA, aging to mimic age-related OA, and collagenase-induced OA (CIOA) to mimic inflammatory OA.

MATERIAL AND METHODS

Animal models

Animal models and controls (ten mice/group) were generated using C57BL/6JR6 males that are known to display more severe and reproducible disease [10] and were supplied by the same company (Janvier Labs, France). *Bscl2*-/- mice (SP-MNX and SP-sham controls; C57BL/6J background) were from CEA (Direction des Sciences du Vivant/Genoscope /LABGEM). Six animals per group were calculated to be required to demonstrate significance at the 5% level with a power of 80% using the G*power software but 10 animals were included to have 6 animals with an OA score ≥ 3 at the end of the experiment. MNX was performed in one joint of 10 weeks old mice by the use of partial meniscectomy as described

[11, 12] and done by a single trained operator in all laboratories. All animal procedures were approved by the local institutions' animal welfare committees and were performed in accordance with the European guidelines for the care and use of laboratory animals (2010/63/UE). Surgery and euthanasia were performed after anaesthesia with isoflurane gas, and all efforts were made to minimize suffering. Mice were housed in solid bottomed plastic cages in quiet rooms at 22° ± 1°C, 60% controlled humidity, and 12h/12h light/dark cycle. Animals were used after an adaptation period of 7 days and had free access to tap water and standard pelleted chow (except the HF model). Mice were sacrificed at week 6 after OA induction to have a comparable disease time induction although we were aware that OA severity can vary according to the model.

- **Joint instability model**

MNX was selected as the reference model of joint instability-related OA [11]. Knee joint instability was induced surgically in the right knee by medial partial meniscectomy. Surgery was performed under a binocular magnifier (X15) using a Sharpoint microsurgical stab knife. Mice were placed in dorsal position, knee flexed and right foot taped. After skin incision, the medial femoro-tibial ligament was cut, a short incision of the medial side of quadriceps muscle was performed, the knee capsule was cleaved and the patella was sub-luxated laterally. After section of the meniscotibial ligament, the medial meniscus was gently pulled out and ¾ of its anterior horn removed. Then, the patella was replaced, the quadriceps muscle and the skin plan sutured. Control animals underwent sham surgery (ligament visualization but not dissection).

- **Hypergravity model**

Hypergravity mimics the overweight-associated mechanical strain on joints without metabolism dysregulation. In mice with MNX, hypergravity induces large OA lesions that are

not observed without surgical induction [13, 14]. MNX was performed on the right knee, and mice were put back in their box for 48 hours. Then, cages were transferred in the gondolas of the centrifuge (COMAT Aérospace, Flourens, France) to maintain a permanent level of hyper gravity [14]. This device has four 1.4m-long arms that hold at their distant end a mobile octagonal gondola (56.2 × 52.0 × 59.2 cm). All gondolas are equipped with an infra-red video surveillance system to monitor the animals' condition and food/water stocks. In the centrifuge, temperature and light conditions were identical to that of control cages. At the start of centrifugation, acceleration was smoothly and gradually increased over a period of 40 sec. The final acceleration was 2 g (29.6 rpm), and animals were kept at 2 g for 6 weeks. Animals were provided with enough food and water for 4 weeks. Then, the centrifuge was transiently stopped to allow litter change, animal weighing, and chow and water supply refilling. Control mice with MNX were not exposed to hypergravity.

- **Metabolic disorder model**

Seipin (SP) knock-out mice are representative of metabolism disorder, which is a feature associated with OA [15]. *Bscl2* deficiency in mice recapitulates the main features of the phenotype of patients with Berardinelli-Seip Congenital Lipodystrophy (BSCL), including almost complete absence of adipose tissue, hyperglycaemia, hyperinsulinemia, and insulin resistance. MNX and Sham surgery were performed in 10 week-old *Bscl2*-/- mice.

- **High Fat Diet model**

The high fat diet model reproduces the effect of obesity and dysregulated metabolism on OA onset [16]. At the age of six weeks, mice were fed with High Fat Diet (HFD, 60% of calories from fat, Ssniff, EF D12492 (II) mod. Soest, Germany) that was provided ad libitum for 10 weeks with the chow changed twice per week. A number of mice 20% higher than the final group size was included to ensure statistical power of the experimentation. MNX was

performed at the age of 10 weeks. In absence of surgical induction, mice did not develop spontaneous lesions of OA. The average weekly weight gain ranged from 1 g to 1.5 g, leading to a final weight gain of 73% (mean: 14.6 g) associated with insulin resistance (HOMA-IR: +246%). Considering the large variability generally observed in the final body weight and fat mass, only animals with a final weight gain higher than 70% were analysed.

- **Collagenase-induced OA model**

The collagenase-induced model (CIOA) is characterized by low grade inflammation of the synovial membrane, leading to OA lesions [10]. A solution of 1 U/5µL type VII collagenase from *Clostridium histolyticum* (Sigma-Aldrich) was prepared in saline solution. At day 0, a small skin incision was performed on top of the patellar tendon. The knee was bended and the collagenase solution (5 µL) was injected in the intra-articular space using a 10 µL syringe (Hamilton) with a 25 gauge needle. On day 2, a second collagenase injection was performed according to the same procedure. Six weeks later, animals were sacrificed. Control animals were injected with saline solution.

- **Age-related model**

Ageing is the main risk OA factor [17]. C57BL/6JRj mice exhibit mild OA lesions in the knee at the age of 18 to 24 months [18]. Mice were housed with free access to food and water and euthanized at the age of 24 months. Control young mice were kept in the animal facility and euthanized at the age of 16 weeks.

Sample preparation for histology and mRNA extraction

After sacrifice, femora and tibiae from 10 knee joints (one joint/mouse) per model were dissected. Skin and muscles were removed and the knee joint was isolated by sectioning the distal extremity of tibiae and proximal part of the femurs. The tibial plateau was isolated

from bone at the growth plate interface, by cutting 2-3 mm beneath the cartilage surface. The remaining soft tissues (meniscus, ligaments and synovium) were removed. The tibial plateau was immediately placed in 1mL of TRIzol® Reagent (Life Technologies), snap-frozen in liquid nitrogen, and stored at -80°C till RNA extraction. After isolation, femoral condyles were fixed in 4% paraformaldehyde for 36 hours, and then decalcified in 0.5M EDTA at room temperature for 15 days.

Histology

After dehydration in a graded series of alcohol, femoral condyles were embedded in paraffin at 60°C in a tissue processor. On average, 30 serial sagittal sections of 5 µm were cut, and three were chosen at the upper, medium and lower levels every 50 µm from cartilage surface. OA scoring was performed after Safranin O-Fast Green staining, according to the OsteoArthritis Research Society International (OARSI) recommendations [19]. For each animal, the OA score was the highest score obtained at one of the three levels. For each model, all sections were blindly scored by the same three readers.

RNA isolation

Tibial plateau samples were prepared in each consortium laboratory and then shipped for centralized RNA extraction that was performed by crushing thawed samples with ceramic beads (Precellys® Lysing kit CK28R), using a Precellys® 24 tissue homogenizer equipped with the Cryolis® cooling unit (Bertin Technologies). Samples underwent three successive lysis cycles at 6500 rpm for 15 sec, spaced by a 5 min lag phase at 4°C, before addition of 200 µL chloroform. After incubation at room temperature for 3 min, the aqueous phase was recovered, 600 µL of 70% ethanol was added, and the solution was transferred to an

RNeasy® spin column (Qiagen) and the next steps were performed according to the supplier's recommendations. Total RNA was quantified with a Nanodrop® instrument and aliquots were frozen at - 80°C. RNA integrity was confirmed with the Agilent® RNA 6000 kit on an Agilent Bioanalyzer 2100®.

Transcriptomic analysis

Transcriptomic analysis was performed on Custom TaqMan® Array Microfluidic Cards (TAC) that were designed to perform 384 real-time PCR reactions on a ViiA™ 7 Fast Real-Time PCR System (Applied Biosystems®). Custom TAC were designed for the analysis of TGFβ family members (table 1). Reverse transcription was performed using 250 ng of total RNA and the High capacity cDNA Reverse Transcription Kit (Life Technologies). Quantitative PCR was done using cDNA (150 ng) mixed with TaqMan Fast Advanced Master Mix (Life Technologies). After 40 cycles of amplification (95°C for 20 sec and then 95°C for 1 sec and 60°C for 20 sec), data were analysed with the Applied Biosystems® Relative Quantification Analysis Module. Amplification curves for each target were individually checked and baselines adjusted, when necessary, to determine the cycle threshold (CT) values. Gene expression was normalized to the mean CT value of four housekeeping genes (*Gusb, Hprt, Rps9, Ppia*) and expressed as relative gene expression using the $2^{-\Delta CT}$ formula or as a fold change expression using the $2^{-\Delta\Delta CT}$ formula.

Statistical analysis

Unsupervised two-dimensional hierarchical clustering was generated with mean-centred relative expression values ($2^{-\Delta Ct}$) of 91 genes per sample using XLStat software. Distances between samples were calculated based on the ΔCT values using Pearson's Correlation and

average linkage method. The vertical height of the dendogram shows the Euclidean distances between samples. The two-dimensional scatter plot of Principal Component Analysis (PCA) was performed using XLStat and represents the expression pattern of ($2^{-\Delta Ct}$) sample values of the ten subgroups. When plotting the sample data points, F1 (PCA Component 1 (32.85% variance)) was used as the x-axis and F2 (PCA Component 2 (12.69% variance)) as the y-axis. Data did not assume a Gaussian distribution and were considered unpaired. The statistical analysis was performed between 2 groups for each OA model versus its respective control (MNX vs MNX-sham, CIOA vs CIOA-sham, Aged vs Young, SP-MNX vs MNX, HG-MNX vs MNX, and HF-MNX vs MNX) using the Mann-Whitney test and GraphPad 7 (San Diego, CA, USA). Data were expressed as relative expression ($2^{-\Delta Ct}$) or as fold change (fold change of gene expression in one OA sample as compared to its respective control normalized to 1) and represented as median with interquartile range. Differences were considered significant at $p<0.05$ and $p<0.01$.

RESULTS

Defining the Standard Operating Procedures. One important feature in the study design was to define the SOP after the harmonization of the experimental protocols (from animal models to transcriptomic analysis) in three consensus meetings of the ROAD consortium. A study workflow was designed (Figure 1). At each step, the analysis technique was performed in a single laboratory by the same operator to avoid experimental bias. The centralized OA scoring of the different models and controls (Figure 2A) showed that OA scores were significantly higher in all models (≥3 on a scale of 0 to 5) than in their respective control (score ≤2), although variability in control samples was observed (Figure 2B). The

concentration of total RNA isolated from tibial plateau samples was not homogeneous among samples, and was significantly higher in the aged, HG-MNX and HF-MNX models than in their controls (young and MNX mice, respectively) (Figure 2C). The RIN score, which estimates RNA quality and integrity, was heterogeneous among samples, with significantly lower scores in samples from the aged and CIOA animals than from their controls (young and CIOA-sham) (Figure 2D). Among all samples, six out of the ten samples per group that met the criteria of selection were analysed by TAC. The mean CT values for the housekeeping genes were significantly higher in the CIOA, HG-MNX and HF-MNX samples than in their controls (Figure 2E). However, the mean CT values for the housekeeping genes were positively correlated with the mean CT values for all genes (Figure 2F). This indicated that the lower expression of housekeeping genes in some samples could be attributed to a lower amount of cDNA loaded in the TAC and not to a differential regulation of the housekeeping genes. We also detected the expression of genes specific for cartilage (type II collagen, aggrecan) or bone (Runx2, Sp7) in all OA models (data not shown), indicating that both tissues were represented in our samples.

TGFβ signatures according to the experimental OA phenotypes. Hierarchical clustering and average linkage clustering of the mRNA expression data in the 10 groups of mice (6 OA models and 4 controls) revealed marked differences among groups (Figure 3A). Three main subgroups could be detected: a cluster that included samples from mice with Aging-, HF-MNX-, HG-MNX-related OA; a cluster that included mainly samples from SP-sham, SP-MNX mice; and a cluster of samples from MNX, CIOA, and CIOA-sham. Sham samples did not cluster together, even though most of them are distributed in the last group with the exception of SP-sham, which is closer to SP-MNX. PCA revealed distinct

transcriptional profiles among groups that allowed gathering them in three distinct clusters (Figure 3B). One (HG-MNX and HF-MNX) was clearly separated from the other two clusters that included i) CIOA, MNX and young animals, and ii) control groups (sham, SP-sham, CIOA-sham). Conversely, old and SP-MNX animals were set apart from the others.

To determine whether a specific gene signature could be associated with the different OA phenotypes, the gene expression profile of each OA group was compared with that of its control: MNX vs MNX-sham, CIOA vs CIOA-sham, Aged vs Young, SP-MNX vs MNX, HG-MNX vs MNX, and HF-MNX vs MNX. The number of significantly deregulated genes was similar in the MNX, SP-MNX, HG-MNX and HF-MNX groups (around 30 genes) (Figure 3C). Conversely, 15 and 47 genes were deregulated in the samples from CIOA and Aged animals, respectively. We identified genes that were common to two or more groups and a gene signature that was specific for each OA model (see Venn diagram in Figure 3D and table 2). Importantly, no gene was deregulated in all six OA models.

OA model-specific TGFβ signatures. To further analyse the specific gene signatures, we visualized the genes that were significantly dysregulated (fold change >1.5) in each OA model using Volcano plots. In the MNX model, gene expression profiling revealed that all 30 modulated genes were upregulated compared with control (Figure 4A). In the CIOA model, 14 of the 15 deregulated genes were significantly upregulated (Figure 4B). Conversely, in the Aging- and SP-MNX-related OA, most genes were downregulated (44/47 and 25/28 genes, respectively) (Figure 4C-D). Finally, in the HG-MNX and HF-MNX models, 70% and 71% of genes were upregulated (Figure 4E-F). Only four genes were differentially regulated between these models: *Smurf2* and *Id2* were upregulated, *Tgfbrap1* and *Lefty* were downregulated only in the HF-MNX model. Altogether, our data revealed that many TGFβ family members

were deregulated in the different OA subtypes, supporting the key role of the TGFβ pathway, whatever the OA risk factor.

A *Gdf5*, *Ltbp4*, *Cd36* combinatorial gene signature for OA. Then, we split the six OA models in two groups. The first group included the OA models related to obesity or fat metabolism (SP-MNX, HG-MNX, and HF-MNX) and/or MNX. The number of shared and specific genes is shown in the Venn diagram (Figure 5A). Most of the modulated genes were common to two or three models, and few genes were specific to each model. However, only *Cd36* was deregulated in all four models. The second group included MNX and the two other most common OA models: inflammation (CIOA) and aging (Figure 5B). Approximately 50% of all deregulated genes were specific to each model and only two genes were deregulated in all three models: *Gdf5* and *Ltbp4*. Analysis of these three genes in all models and their respective controls showed that *Cd36* was significantly upregulated in MNX, SP-MNX, HG-MNX and HF-MNX samples (Figure 5C). *Gdf5* was significantly upregulated in the MNX and CIOA models and significantly downregulated in the Aging model. *Ltbp4* was significantly upregulated in all models, but for the Aging model where it was significantly downregulated. These data suggest that *Cd36* upregulation is a hallmark of trauma-related OA, while the deregulation of *Gdf5* and *Ltbp4* is related to different OA stimuli.

DISCUSSION

The first objective of the ROAD consortium was to identify specific gene signatures for the main OA clinical phenotypes using six relevant murine models by focusing on the

transcriptomic analysis of the TGFβ pathway. Although this pathway has been extensively studied in some OA murine models [18, 20, 21], it is quite impossible to compare these results from independent laboratories due to potential biases that may influence gene expression, such as mouse genetic background, age, sex, housing conditions, histopathological scoring subjectivity and inter-investigator variability. Here, we wanted to limit these potential biases by defining SOPs and by centralizing each step of data acquisition and processing, thereby minimizing the risks of failure to identify relevant targets [22-25]. The resulting data allowed the accurate comparative analysis of six models using their respective controls.

The main finding of our transcriptomic analysis is the unexpected lack of deregulated genes common to all murine models of OA, although many TGFβ family members were deregulated pointing out the critical role played by the TGFβ pathway in OA [26]. This might reflect the heterogeneity of responses to the different stimuli leading to similar symptoms, as observed in patients with OA. Differences in the expression pattern between the different models likely relate to the peculiarities and distinct natures of the models. We are also aware that transcriptional regulation of genes may not be reflected at the protein level. Analysis of these differences at the protein level were beyond the scope of the present study but likely warrants further studies. Some genes, such as type II collagen, may be differently regulated depending on the OA model suggesting possible different timings or mechanisms of regulation that warrant further investigation. Heterogeneity may also be emphasized by the individual responses within the same model, thus highlighting the interest of classifying OA phenotypes using relevant biomarkers in the clinic. Heterogeneity might also reflect different stages of OA in the different models but this is unlikely since the OA scores are similar in all models. The

absence of a common signature could also be due to the late time point (6 weeks after OA induction and 24 months of age for old mice) chosen for the transcriptomic analysis when the gene expression profile might reflect an adaptive response. However, this time point is relevant for patients in whom OA is generally diagnosed long after disease initiation.

Another important finding is the identification of the combinatorial *Gdf5-Cd36-Ltbp4* signature that might discriminate distinct subgroups of OA phenotypes. Indeed, *Cd36* was upregulated in all mice that underwent surgical MNX. CD36 is a membrane-bound protein and the receptor of thrombospondin-1, fatty acid translocase (FAT), platelet glycoprotein 4 (PG4) and scavenger receptor class B member 3 (SCARB3). It is expressed in adipocytes and mesenchymal stromal cells isolated from fat tissue, and its expression level correlates with poor differentiation into the chondrogenic lineage [27]. CD36 expression is increased at sites of cartilage injury and co-localizes with developing hypertrophic chondrocytes and the aggrecan NITEGE neo-epitope [28]. In patients with OA, CD36 expression has been significantly associated with the presence of osteophytes, of joint space narrowing, and higher Kellgren-Lawrence score [29]. Moreover, in chondrocytes from patients with OA, expression of thrombospondin 1 (a CD36 ligand) is strongly decreased concomitantly with the increase in CD36 expression [30]. More recently, the anti-inflammatory and analgesic effects of serum albumin in patients with knee OA was related to inhibition of CD36 in synoviocytes, macrophages and chondrocytes [31]. In addition, our study suggests that CD36 might be a specific biomarker of post-traumatic OA. CD36 expression should be thoroughly investigated in cartilage and bone samples from patients with different OA phenotypes.

We also found that *Gdf5* expression was deregulated in three of the six OA models under study. It was previously shown that a loss-of-function *GDF5* gene mutation results in joint fusions, and a single-nucleotide polymorphism is associated with higher

susceptibility to OA [32]. GDF5 deficiency has also been associated with abnormal ligament laxity and subchondral bone remodelling [33]. Several genome-wide association studies (GWAS) have reported the significant association between knee OA and the *GDF5* locus [29, 34-36]. Very recently, a GWAS using the United Kingdom OA Biobank cohort reported that *GDF5* genetic variants were the strongest predictor of knee pain [37]. In the present study, *Gdf5* expression was upregulated in the CIOA and MNX models that are characterized by ligament laxity and pain [10, 38]. Our data strongly suggest that GDF5 expression is a biomarker of painful OA phenotypes, as also suggested by genomic studies in humans.

Finally, we found that *Ltbp4* was deregulated in all six OA models (Figure 5C), although it was not identified as a deregulated gene common to all models in the statistical analysis (Figure 3D). In the bioinformatic analysis, SP-MNX samples were compared with MNX samples (Figure 4) to investigate the impact of the genetic background on OA. Conversely, in the data presented in Figure 5C, all groups were analysed independently of their control. LTBP4 is a key molecule required for the stability of the TGFβ receptor (TGFβR) complex via interaction with TGFβR2, thereby preventing its endocytosis and lysosomal degradation [39]. However, LTBP4 has not been associated with cartilage or OA and unlike its paralogues, LTBP4 is not regulated during chondrogenic differentiation of mesenchymal stromal cells [40]. Like *Gdf5*, *Ltbp4* expression was decreased in old mice and not upregulated as observed in the murine models of induced OA. This suggests that spontaneous aging-related OA might involve different mechanisms.

In conclusion, the originality of the present study was to rely on relevant murine models of OA to understand the complexity of OA phenotypes in humans through investigation of the TGFβ pathway and based on rigorous SOPs. We did not identify a unique gene signature

common to all six OA phenotypes. This highlights the huge heterogeneity of the animal models and the need of caution when extrapolating results from one model to another. But this also highlights that the diversity of the mouse models likely reflects the heterogeneity in human OA. Further studies are needed to validate these potential signatures.

ACKNOWLEDGMENTS

Authors acknowledge Sandy Van Eegher (ROAD consortium) for her helpful contribution to ROAD, Laure Sudre and Audrey Pigenet (Centre de Recherche Saint-Antoine) for histology and Meriem Koufany (iMPOA) for her expert technical assistance. Thanks to the UTE Platform (SFR François Bonamy, FED 4203/ Inserm UMS 016/CNRS 3556) who provided daily care to the animals, and to J. Lesoeur and M. Dutilleul from the SC3M platform (INSERM - U1229 RMeS, SFR François Bonamy, FED 4203/Inserm UMS 016/CNRS 3556, CHU Nantes) for histology in the age-related OA model. Authors also thank the “Réseau d’Histologie Expérimentale de Montpellier” histology facility for tissue processing and the “SMARTY platform and Network of Animal facilities of Montpellier“.

AUTHOR CONTRIBUTIONS

All authors were involved in revising critically the manuscript and approved the final version. MM: Data analysis, manuscript writing; DN: Experiment design, data analysis, manuscript writing; HKE, DM, MR, EH, XH, DC, MCS, CJa, JYJ, MHLP, PR, JS, CV: Experimental work; FR, CJo, JG, FB: Experiment design, manuscript writing.

ROLE OF THE FUNDING SOURCE

Authors would like to thank the Fondation Arthritis that sponsored the network called ROAD (Research on OsteoArthritis Diseases) that included the seven academic French laboratories involved in this study. The sponsor had no role in the study design or in the collection, analysis or interpretation of the data. DM was granted a contrat d'interface by the Centre Hospitalier Régional Universitaire of Nancy.

COMPETING INTERESTS

The authors declare that they have no competing interests.

REFERENCES

1. Dell'Isola A, Allan R, Smith SL, Marreiros SS, Steultjens M. Identification of clinical phenotypes in knee osteoarthritis: a systematic review of the literature. BMC Musculoskelet Disord 2016; 17: 425.
2. van der Esch M, Knoop J, van der Leeden M, Roorda LD, Lems WF, Knol DL, et al. Clinical phenotypes in patients with knee osteoarthritis: a study in the Amsterdam osteoarthritis cohort. Osteoarthritis Cartilage 2015; 23: 544-549.
3. Waarsing JH, Bierma-Zeinstra SM, Weinans H. Distinct subtypes of knee osteoarthritis: data from the Osteoarthritis Initiative. Rheumatology (Oxford) 2015; 54: 1650-1658.
4. Van Spil WE, Kubassova O, Boesen M, Bay-Jensen AC, Mobasheri A. Osteoarthritis phenotypes and novel therapeutic targets. Biochem Pharmacol 2019; 165: 41-48.
5. Deveza LA, Nelson AE, Loeser RF. Phenotypes of osteoarthritis: current state and future implications. Clin Exp Rheumatol 2019; 37 Suppl 120: 64-72.
6. Ajekigbe B, Cheung K, Xu Y, Skelton AJ, Panagiotopoulos A, Soul J, et al. Identification of long non-coding RNAs expressed in knee and hip osteoarthritic cartilage. Osteoarthritis Cartilage 2019; 27: 694-702.
7. Ji Q, Zheng Y, Zhang G, Hu Y, Fan X, Hou Y, et al. Single-cell RNA-seq analysis reveals the progression of human osteoarthritis. Ann Rheum Dis 2019; 78: 100-110.
8. Sebastian A, Chang JC, Mendez ME, Murugesh DK, Hatsell S, Economides AN, et al. Comparative Transcriptomics Identifies Novel Genes and Pathways Involved in Post-Traumatic Osteoarthritis Development and Progression. Int J Mol Sci 2018; 19.
9. van der Kraan PM. The changing role of TGFbeta in healthy, ageing and osteoarthritic joints. Nat Rev Rheumatol 2017; 13: 155-163.
10. Fang H, Beier F. Mouse models of osteoarthritis: modelling risk factors and assessing outcomes. Nat Rev Rheumatol 2014; 10: 413-421.
11. Kadri A, Ea HK, Bazille C, Hannouche D, Liote F, Cohen-Solal ME. Osteoprotegerin inhibits cartilage degradation through an effect on trabecular bone in murine experimental osteoarthritis. Arthritis Rheum 2008; 58: 2379-2386.
12. Kamekura S, Hoshi K, Shimoaka T, Chung U, Chikuda H, Yamada T, et al. Osteoarthritis development in novel experimental mouse models induced by knee joint instability. Osteoarthritis Cartilage 2005; 13: 632-641.
13. Bojados M, Jamon M. The long-term consequences of the exposure to increasing gravity levels on the muscular, vestibular and cognitive functions in adult mice. Behav Brain Res 2014; 264: 64-73.
14. Gnyubkin V, Guignandon A, Laroche N, Vanden-Bossche A, Normand M, Lafage-Proust MH, et al. Effects of chronic hypergravity: from adaptive to deleterious responses in growing mouse skeleton. J Appl Physiol (1985) 2015; 119: 908-917.
15. Prieur X, Dollet L, Takahashi M, Nemani M, Pillot B, Le May C, et al. Thiazolidinediones partially reverse the metabolic disturbances observed in Bscl2/seipin-deficient mice. Diabetologia 2013; 56: 1813-1825.
16. Gallou-Kabani C, Vige A, Gross MS, Rabes JP, Boileau C, Larue-Achagiotis C, et al. C57BL/6J and A/J mice fed a high-fat diet delineate components of metabolic syndrome. Obesity (Silver Spring) 2007; 15: 1996-2005.
17. Hunter DJ, Bierma-Zeinstra S. Osteoarthritis. Lancet 2019; 393: 1745-1759.
18. Stanescu R, Knyszynski A, Muriel MP, Stanescu V. Early lesions of the articular surface in a strain of mice with very high incidence of spontaneous osteoarthritic-like lesions. J Rheumatol 1993; 20: 102-110.
19. Glasson SS, Chambers MG, Van Den Berg WB, Little CB. The OARSI histopathology initiative - recommendations for histological assessments of osteoarthritis in the mouse. Osteoarthritis Cartilage 2010; 18 Suppl 3: S17-23.

20. Blaney Davidson EN, Vitters EL, Bennink MB, van Lent PL, van Caam AP, Blom AB, et al. Inducible chondrocyte-specific overexpression of BMP2 in young mice results in severe aggravation of osteophyte formation in experimental OA without altering cartilage damage. Ann Rheum Dis 2015; 74: 1257-1264.
21. Cui Z, Crane J, Xie H, Jin X, Zhen G, Li C, et al. Halofuginone attenuates osteoarthritis by inhibition of TGF-beta activity and H-type vessel formation in subchondral bone. Ann Rheum Dis 2016; 75: 1714-1721.
22. Ma HL, Blanchet TJ, Peluso D, Hopkins B, Morris EA, Glasson SS. Osteoarthritis severity is sex dependent in a surgical mouse model. Osteoarthritis Cartilage 2007; 15: 695-700.
23. Rai MF, Sandell LJ. Regeneration of articular cartilage in healer and non-healer mice. Matrix Biol 2014; 39: 50-55.
24. Maynard CL, Elson CO, Hatton RD, Weaver CT. Reciprocal interactions of the intestinal microbiota and immune system. Nature 2012; 489: 231-241.
25. Bello S, Krogsboll LT, Gruber J, Zhao ZJ, Fischer D, Hrobjartsson A. Lack of blinding of outcome assessors in animal model experiments implies risk of observer bias. J Clin Epidemiol 2014; 67: 973-983.
26. van der Kraan PM. Differential Role of Transforming Growth Factor-beta in an Osteoarthritic or a Healthy Joint. J Bone Metab 2018; 25: 65-72.
27. Alegre-Aguaron E, Desportes P, Garcia-Alvarez F, Castiella T, Larrad L, Martinez-Lorenzo MJ. Differences in surface marker expression and chondrogenic potential among various tissue-derived mesenchymal cells from elderly patients with osteoarthritis. Cells Tissues Organs 2012; 196: 231-240.
28. Cecil DL, Appleton CT, Polewski MD, Mort JS, Schmidt AM, Bendele A, et al. The pattern recognition receptor CD36 is a chondrocyte hypertrophy marker associated with suppression of catabolic responses and promotion of repair responses to inflammatory stimuli. J Immunol 2009; 182: 5024-5031.
29. Valdes AM, Hart DJ, Jones KA, Surdulescu G, Swarbrick P, Doyle DV, et al. Association study of candidate genes for the prevalence and progression of knee osteoarthritis. Arthritis Rheum 2004; 50: 2497-2507.
30. Pfander D, Cramer T, Deuerling D, Weseloh G, Swoboda B. Expression of thrombospondin-1 and its receptor CD36 in human osteoarthritic cartilage. Ann Rheum Dis 2000; 59: 448-454.
31. Bar-Or D, Thomas G, Rael LT, Frederick E, Hausburg M, Bar-Or R, et al. On the mechanisms of action of the low molecular weight fraction of commercial human serum albumin in osteoarthritis. Curr Rheumatol Rev 2018.
32. Miyamoto Y, Mabuchi A, Shi D, Kubo T, Takatori Y, Saito S, et al. A functional polymorphism in the 5' UTR of GDF5 is associated with susceptibility to osteoarthritis. Nat Genet 2007; 39: 529-533.
33. Thysen S, Luyten FP, Lories RJ. Targets, models and challenges in osteoarthritis research. Dis Model Mech 2015; 8: 17-30.
34. Valdes AM, Evangelou E, Kerkhof HJ, Tamm A, Doherty SA, Kisand K, et al. The GDF5 rs143383 polymorphism is associated with osteoarthritis of the knee with genome-wide statistical significance. Ann Rheum Dis 2011; 70: 873-875.
35. Yau MS, Yerges-Armstrong LM, Liu Y, Lewis CE, Duggan DJ, Renner JB, et al. Genome-Wide Association Study of Radiographic Knee Osteoarthritis in North American Caucasians. Arthritis Rheumatol 2017; 69: 343-351.
36. Zhang R, Yao J, Xu P, Ji B, Luck JV, Chin B, et al. A comprehensive meta-analysis of association between genetic variants of GDF5 and osteoarthritis of the knee, hip and hand. Inflamm Res 2015; 64: 405-414.
37. Meng W, Adams MJ, Palmer CNA, andMe Research T, Shi J, Auton A, et al. Genome-wide association study of knee pain identifies associations with GDF5 and COL27A1 in UK Biobank. Commun Biol 2019; 2: 321.

38. Bapat S, Hubbard D, Munjal A, Hunter M, Fulzele S. Pros and cons of mouse models for studying osteoarthritis. Clin Transl Med 2018; 7: 36.
39. Su CT, Huang JW, Chiang CK, Lawrence EC, Levine KL, Dabovic B, et al. Latent transforming growth factor binding protein 4 regulates transforming growth factor beta receptor stability. Hum Mol Genet 2015; 24: 4024-4036.
40. Goessler UR, Bugert P, Bieback K, Deml M, Sadick H, Hormann K, et al. In-vitro analysis of the expression of TGFbeta -superfamily-members during chondrogenic differentiation of mesenchymal stem cells and chondrocytes during dedifferentiation in cell culture. Cell Mol Biol Lett 2005; 10: 345-362.

FIGURE LEGENDS

Fig. 1. Study workflow. Samples were collected from six OA models and their respective controls: OA induced by Destabilization of the Medial Meniscus (MNX) versus sham, OA associated with age (Ageing) versus young animals, inflammation (Collagenase-induced OA; CIOA) versus sham, obesity [High Fat (HF) versus Normal Diet (ND)] overweight [Hypergravity (HG-MNX) versus MNX] (these models were generated in C57BL/6JRj male mice), and OA associated with metabolic syndrome (Seipin knock-out; SP-MNX versus SP-sham). At the experiment end, knee joints were harvested; femoral condyles and tibial plateaus were prepared for histological analyses and RNA isolation, respectively. OA severity was scored after Safranin-O-Fast Green staining using the OARSI grading system. The expression of genes involved in TGF-β signalling was analysed using custom-made Taqman™ Array Cards.

Fig. 2. Sample quality controls. **(A)** Sagittal views of femoral condyles from CIOA-sham (left) and CIOA (right) mice as representative of control and OA cartilage (OA score= 1 and 4, respectively). **(B)** Distribution of OARSI scores for cartilage destruction in histological sections of femoral condyles. Results are presented as median with interquartile range (n=6). **(C)** Total RNA concentration (ng/µL) after extraction from tibial plateau samples of OA models and controls. **(D)** RNA Integrity Number (RIN) for total RNA extracted from tibial plateau samples of OA models and controls. **(E)** Mean CT values for the housekeeping genes *Ppia*, *Hprt*, *Gusb*, and *Rps9* obtained using Taqman® Array Cards. Data are represented as median with interquartile range; *p <0.05, **p <0.01 (Mann-Whitney test). **(F)** Correlation between the mean CT value of the four housekeeping genes and the mean CT value of all genes. Each dot represents a sample (n=59): Pearson's r=0.8471, p <0.001.

Fig. 3. Global gene expression analysis. **(A)** Unsupervised hierarchical clustering (Pearson correlation, average linkage) of the six samples for each OA model and for each of the four controls. **(B)** Principal component analysis of the same data as in A. Squares represent the centroid of each group (n=6 mice per group). **(C)** Number of significantly deregulated genes in the six OA murine models compared with their controls. **(D)** Venn diagram showing the number of significantly deregulated genes identified in each OA models in a set of 91 targets (Table 1).

Fig. 4. Analysis of differentially expressed genes in the OA murine models. Results are shown for DMM **(A)**, CIOA **(B)**, Ageing **(C)**, SP-DMM **(D)**, HG-DMM **(E)** and HF-DMM **(F)**. Volcano plots (left panels) show the up- and downregulated genes in each OA model versus its control. For each plot, the x-axis represents the log 2-fold change (FC), and the y-axis represents the log 10 p-values. Genes with an exact p-value <0.05 were considered as differentially expressed. Scatter plots (right panels) show the expression FC of significantly deregulated genes ($p<0.05$) in the six OA models compared with their control group. Results are expressed as the median with interquartile range (n=6).

Fig. 5. Genes significantly deregulated in the various OA models. **(A)** Venn diagrams showing the number of differentially expressed genes identified in the four OA models related to overweight or metabolism disorder (MNX, SP-MNX, HG-MNX, HF-MNX), and **(B)** in the three most common OA models (MNX, CIOA, Aged), among a set of 92 targets (Table 1). **(C)** Relative gene expression of *Cd36, Gdf5, Ltbp4* in the four controls and six OA models are

expressed as the median with interquartile range (n=6/group); * p <0.05, ** p <0.01 (Mann-Whitney test).

Supplementary Fig. Representative photographs of sagittal histological sections of femoral condyles from the different OA models.